

Interface scattering and resistivity of fiber-reinforced metal-matrix composites

Curt A. Moyer

Department of Physics and Center for Advanced Materials Processing, Clarkson University, Potsdam, New York 13699

(Received 3 June 1992)

An analytical approach to assessing the contribution to the resistivity of metal-matrix composites resulting from electrons scattering from the surface of the embedded phase is described. Results are presented for conduction along the fiber axis which do not imply any substantial enhancement of resistivity at low temperature, contrary to earlier predictions (but consistent with recent experiments). The scattering effect on conduction transverse to the fiber axis is investigated using an extension of the model originally proposed by Rayleigh. The magnitude of the scattering correction is found to be comparable to that in the longitudinal orientation, and does not account for the abnormally high transverse resistivity reported for B-Al composites containing 60% boron fiber by volume. A possible explanation and remedy for the discrepancy is discussed.

I. INTRODUCTION

The theory of composites attempts to assign to a multi-phase (heterogeneous) material an effective physical property like conductivity, given the properties of the component (homogeneous) phases, and their morphology. More sophisticated treatments also address special considerations that arise specifically from the mixed phase—the decrease in conductivity expected from carrier scattering at the phase boundaries is one example. Such effects clearly demonstrate that a composite specimen is more than just the sum of its parts, and have led to important new classes of materials.

This work is motivated by two developments, one experimental and the other theoretical. The former are measurements for the resistivity of various B-Al composites from room temperature down to the boiling point of liquid nitrogen. For samples containing more than about 48% boron fiber by volume, the temperature variation of resistivity is anomalous and decreases at a rate slower than expected for the metal matrix. And in one case (60% fiber content), the transverse and longitudinal resistivities actually obey *different* temperature laws.¹ This behavior, inexplicable in terms of the component properties alone, clearly signals some sort of interface effect. Indeed, the data are qualitatively consistent with an additional contribution to the sample resistivity arising from scattering at the fiber-metal boundary.

A theory for interface scattering in metal-matrix composites was given recently by Roig and Schoutens.² At very low temperatures (below 10 K), they predict a rise in resistivity, which, however, does not appear to be in accord with experiment.³ Furthermore, their resistivity calculations are limited to the *longitudinal* configuration, where current flows parallel to the fiber axis. In Sec. II and III that follow, we reexamine the theoretical problem of interface scattering in metal-matrix composites, and present results for both the longitudinal and transverse cases. These results are examined in the light of previous theoretical work and the resistivity data for B-Al composites.

Our treatment builds on a companion publication

where we have shown that scattering at the fiber-metal boundary can be seen as producing a local conductivity $\vec{\sigma}(\mathbf{r})$, which grows steadily to become the matrix (metal) value σ_0 far from the fiber surface.⁴ The specific form of $\vec{\sigma}(\mathbf{r})$ is shown in Ref. 4 to be

$$\begin{aligned}\sigma_{\parallel}(\mathbf{r}) &= \sigma_0 \left\{ 1 - \frac{3}{8\pi} [E_2(z) - E_4(z)] \right\}, \\ \sigma_{\perp}(\mathbf{r}) &= \sigma_0 \left\{ 1 - \frac{3}{2} E_4(z) \right\}\end{aligned}\quad (1)$$

for current flow parallel (\parallel) and normal (\perp) to the interface, respectively. Here the E_n are exponential integral functions of argument $z = d(\mathbf{r})/\lambda$, where λ is the mean free path in the bulk, and $d(\mathbf{r})$ is the distance from the field point \mathbf{r} to the interface along a surface normal. This characterization of interface scattering in terms of an effective local conductivity is well suited to composite calculations. In this paper we will use Eq. (1) to obtain an expression for the conductivity of fiber-reinforced metal-matrix composites which includes the effects of scattering at the fiber-metal boundary.

Since the composites in question are highly anisotropic, current flows more readily along the nominal-fiber direction (longitudinal case) than normal to it (transverse case). As noted above, the effects of interface scattering on the longitudinal conductivity have been studied before, but with suspect results; corresponding results for the transverse conductivity have not, to our knowledge, appeared previously.

II. THE LONGITUDINAL CONDUCTIVITY

We envision applications to continuous fiber-reinforced metal-matrix composites which have a well-defined and regular geometry (the B-Al system is such an example). Accordingly, we consider here one of the so-called *lattice models*, consisting of a regular square array of nonconducting circular cylinders (the fibers) embedded in an infinite host (the metal matrix). Figure 1 shows a representative cross section of this material. Each primi-

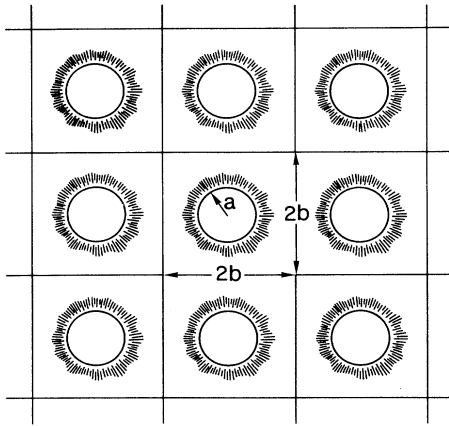


FIG. 1. Lattice model for a fiber-reinforced metal-matrix composite having well-defined and regular geometry. The fibers are represented by circular cylinders with radius a arranged in square order; $2b$ is the separation between fiber centers.

tive cell (square) has edge length $2b$ and contains a fiber of radius a at its center. In the longitudinal orientation, a uniform field \mathbf{E} exists everywhere parallel to the cylinder axis, and current flows normal to the plane of the figure. Yet on account of interface scattering, $\mathbf{J}(\mathbf{r})$ is nonuniform over the cell cross section and the *apparent* longitudinal conductivity σ_l of the specimen becomes

$$\sigma_l = \frac{1}{|\mathbf{E}|A} \int_{A_c} \mathbf{J}_{\parallel}(\mathbf{r}) dA = \frac{1}{A} \int_{A_c} \sigma_{\parallel}(\mathbf{r}) dA, \quad (2)$$

The integrals in Eq. (2) are taken over the cross section A_c with area A , for a single cell (square). The symmetry of the square can be used to reduce the integrals to the first octant. Then, in polar coordinates (r, θ) centered on the cylinder axis we see that $d(\mathbf{r}) = r - a$ and Eq. (2) becomes

$$\frac{\sigma_l}{\sigma_0} = 1 - \frac{\pi a^2}{4b^2} - \frac{3\lambda}{4\pi b^2} \int_0^{\pi/4} d\theta \int_0^{z_c} (\lambda z + a)[E_2(z) - E_4(z)] dz, \quad (3)$$

where $z_c(\theta) = (b \sec \theta - a)/\lambda$ delineates the outer boundary of the cell in z space. Since the volume fraction of fiber in our model is $p = \pi a^2/4b^2$, the first two terms on the right-hand side of Eq. (3) comprise the matrix volume fraction, and give the conductivity expected from the rule of mixtures; the remaining term can be regarded as the correction to p —say δp —resulting from the effects of boundary scattering. To compute δp we first do the integrals over z with the help of the identities

$$\begin{aligned} \frac{dE_n(z)}{dz} &= -E_{n-1}(z), \\ zE_n(z) &= e^{-z} = nE_{n+1}(z) \end{aligned} \quad (4)$$

to get

$$\begin{aligned} \int_0^{z_c} (\lambda z + a)[E_2(z) - E_4(z)] dz \\ = 2\lambda[E_4(z_c) - 2E_6(z_c) + \frac{1}{15}] \\ + a[E_5(z_c) - E_3(z_c) + \frac{1}{4}]. \end{aligned} \quad (5)$$

We have not found a way to carry out the remaining integral over θ exactly, but progress can be made in the extreme limit $\lambda \ll b$. This limitation is fully consistent with Eq. (1), where a mean free path much smaller than a fiber diameter was assumed. We appeal to the integral representation for the functions E_n

$$E_n(z) = \int_1^{\infty} e^{-zt} \frac{dt}{t^n} \quad (6)$$

to write the integral of a typical term in Eq. (5) as

$$\begin{aligned} \int_0^{\pi/4} E_n(z_c) d\theta \\ = \int_1^{\infty} \frac{dt}{t^n} e^{at/\lambda} \int_0^{\pi/4} e^{-bt \sec \theta/\lambda} d\theta \\ = \int_1^{\infty} \frac{dt}{t^n} e^{-[(b-a)/\lambda]t} \\ \times \int_0^{\sqrt{2}-1} e^{-(bt/\lambda)u} \frac{du}{(u+1)\sqrt{u(u+2)}}. \end{aligned} \quad (7)$$

For $\lambda \ll b$ the main contribution to the last integral on the right-hand side comes from the lower limit. Putting $u=0$ in the denominator (but not under the root) and extending the upper limit of integration to infinity gives

$$\begin{aligned} \int_0^{\pi/4} E_n(z_c) d\theta \approx \sqrt{\pi\lambda/b} \int_1^{\infty} e^{-[(b-a)/\lambda]t} \frac{dt}{t^{n+1/2}} \\ \equiv \sqrt{\pi\lambda/b} \mathcal{J}_n \left[\frac{b-a}{\lambda} \right]. \end{aligned} \quad (8)$$

In writing the second line of Eq. (8) we have used the integral to define new functions \mathcal{J}_n closely related to the exponential integral functions E_n [cf. Eq. (6)]. Indeed, the \mathcal{J}_n obey similar recurrence relations [replace n in Eq. (4) with $n + \frac{1}{2}$] but, unlike E_0 , which is an elementary function, \mathcal{J}_0 is related to the complimentary error function:

$$\mathcal{J}_0(z) = \int_1^{\infty} e^{-zt} \frac{dt}{\sqrt{t}} = \sqrt{\pi/z} \operatorname{erfc}(\sqrt{z}). \quad (9)$$

It follows that σ_l can be expressed entirely in terms of elementary functions and the complement of the error function. However, the only simple result is that which obtains if we also insist on $\lambda \ll b - a$:

$$\frac{\sigma_l}{\sigma_0} = 1 - \frac{\pi a^2}{4b^2} - \frac{\pi a^2}{4b^2} \frac{1}{10\pi} \left[\left(\frac{\lambda}{a} \right)^2 + \frac{15}{8} \frac{\lambda}{a} \right]. \quad (10)$$

This last restriction on λ effectively limits Eq. (10) to low fiber concentrations and/or moderate temperatures. To transcend this limitation we must compute the conductivity as $\sigma_l/\sigma_0 = 1 - p - \delta p$ with

$$\frac{\delta p}{p} = \frac{3\lambda}{\pi^2 a} \left\{ \frac{\pi}{16} + \sqrt{\pi\lambda/b} [\mathcal{J}_5(z) - \mathcal{J}_3(z)] \right\} + \frac{6\lambda^2}{\pi^2 a^2} \left\{ \frac{\pi}{60} + \sqrt{\pi\lambda/b} [\mathcal{J}_4(z) - 2\mathcal{J}_6(z)] \right\}. \quad (11)$$

Figure 2 shows $\delta p/p$ as a function of $k=2a/\lambda$ computed from the more accurate Eq. (11) for fiber volume fractions $p=0.3$ and 0.6 . The indistinguishability of the two curves above $k \approx 30$ indicates the simpler Eq. (10) is valid in this regime. For smaller values of k the scattering correction eventually saturates, in contrast to the (erroneous) predictions of Ref. 2.

In the application to B-Al composites, fiber diameters are often several hundred micrometers while the mean free path at ordinary temperatures is less than $1 \mu\text{m}$. Thus $k \sim 100$ for these systems and decreases with decreasing temperature (increasing λ). Inspection of Fig. 2 shows that the scattering correction is typically less than 1% of p but, interestingly, actually tends to be a *smaller* percentage at the higher volume fractions. This feature is absent from previous theories, though consistent with the data on B-Al composites. In particular, Tse¹ has combined longitudinal conductivity data for B-Al composites with the rule of mixtures to deduce resistivity values for the metal matrix. The calculated values tend to run higher than expected, but agreement improves noticeably when the volume concentration of fiber reaches the 60% level.

III. THE TRANSVERSE CONDUCTIVITY

In finding the transverse conductivity of the specimen we follow closely the classic work of Rayleigh,⁵ who solved a similar problem. Below we generalize Rayleigh's

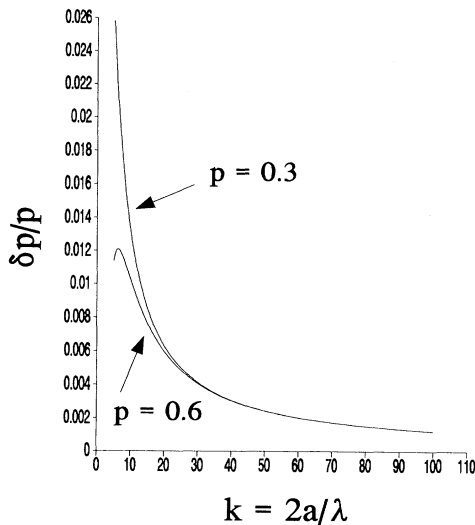


FIG. 2. Scattering correction to the longitudinal conductivity σ_l as a function of $k=2a/\lambda$ for composites with 30% and 60% fiber by volume. The composite conductivity is $\sigma_l/\sigma_0 = 1 - p - \delta p$.

work to include a matrix with continuously varying conductivity to account for the effects of interface scattering.

For the computation of the transverse conductivity σ_t , we take the applied field in the plane of Fig. 1 along the top (or bottom) edge of the representative cell. From the symmetry of the arrangement, it follows that the left and right cell boundaries are equipotentials, while those at the top and bottom are lines of flow. Even without interface scattering, the current density in the matrix $\mathbf{J}(\mathbf{r})$ is nonuniform; the scattering effect complicates the problem further by giving rise to a matrix conductivity $\vec{\sigma}(\mathbf{r})$, which rises steadily in any radial direction from the central cylinder. We assume $\vec{\sigma}(\mathbf{r})$ saturates at the bulk value σ_0 before the representative cell boundary is reached, thereby preserving the individuality of each cell.

Now $\mathbf{J}(\mathbf{r})$ must satisfy the steady state condition $\nabla \cdot \mathbf{J} = 0$. In terms of the electric potential $V(\mathbf{r})$, this is

$$0 = \nabla \cdot [\boldsymbol{\sigma}(\mathbf{r}) \nabla V] = \frac{1}{r} \frac{\partial}{\partial r} \left\{ r \sigma_{\perp} \frac{\partial V}{\partial r} \right\} + \frac{\sigma_{\parallel}}{r^2} \frac{\partial^2 V}{\partial \theta^2}. \quad (12)$$

To begin, we make no distinction between σ_{\perp} and σ_{\parallel} ; subsequently, the results will be modified to account for the tensor character of $\vec{\sigma}$ as given by Eq. (1).

Since the conductivity $\vec{\sigma}(\mathbf{r})$ has the same value at all points \mathbf{r} equidistant from the fiber axis, we imagine dividing the cell of Fig. 1 into annular regions of width Δr . Within the i th such ring σ is nearly constant at the value $\sigma^{(i)}$; accordingly, the electric potential $V^{(i)}$ in this ring satisfies Laplace's equation, and is given in polar coordinates by

$$V^{(i)} = A_0^{(i)} + \sum_{n \text{ odd}}^{\infty} [A_n^{(i)} r^n + B_n^{(i)} r^{-n}] \cos n \theta. \quad (13)$$

The sines of θ and its multiples are excluded by the reflection symmetry about $\theta=0$, and the cosines of the even multiples by reflection symmetry about $\theta=\pi/2$. At the boundary separating adjacent rings the potential must be continuous:

$$A_n^{(i)} r^n + B_n^{(i)} r^{-n} = A_n^{(i+1)} r^n + B_n^{(i+1)} r^{-n} \quad (n \neq 0), \quad (14)$$

$$A_0^{(i)} = A_0^{(i+1)} \quad (n = 0).$$

Across this same boundary, the normal component of $\mathbf{J}(\mathbf{r})$ must also be continuous:

$$\sigma^{(i)} [n A_n^{(i)} r^{n-1} - n B_n^{(i)} r^{-n-1}] = \sigma^{(i+1)} [n A_n^{(i+1)} r^{n-1} - n B_n^{(i+1)} r^{-n-1}] \quad (n \neq 0). \quad (15)$$

We now regard $A_n^{(i)}$, $B_n^{(i)}$ as values taken in the i th ring by continuous functions $A_n(r)$ and $B_n(r)$, respectively, and pass to the continuum limit, where the number of rings increases without bound and their width simultaneously shrinks to zero. After some manipulation, we find in place of Eqs. (14) and (15) the equivalent differential relations

$$\begin{aligned}\frac{\partial A_0}{\partial r} &= 0, \\ \frac{\partial A_n}{\partial r} &= \frac{1}{2\sigma} \frac{\partial \sigma}{\partial r} [r^{-2n} B_n(r) - A_n(r)] \quad (n \neq 0), \\ \frac{\partial B_n}{\partial r} &= \frac{1}{2\sigma} \frac{\partial \sigma}{\partial r} [r^{2n} A_n(r) - B_n(r)] \quad (n \neq 0).\end{aligned}\quad (16)$$

In this limit, the electric potential everywhere inside the metal matrix is given by

$$V(r, \theta) = A_0 + \sum_{n \text{ odd}}^{\infty} [A_n(r)r^n + B_n(r)r^{-n}] \cos n\theta, \quad (17)$$

with $A_n(r)$ and $B_n(r)$ obeying Eqs. (16). It is a straightforward exercise to show that Eqs. (16) and (17) are fully consistent with the steady-state requirement Eq. (12) for a scalar conductivity $\sigma(r)$.

To accommodate the tensor conductivity of Eq. (1), we retain the prescriptions of Eqs. (16) but allow Eq. (12) to fix the correct effective scalar conductivity $\sigma(r)$. The result

$$\frac{1}{\sigma} \frac{\partial \sigma}{\partial r} = \frac{1}{\sigma_{\perp}} \frac{\partial \sigma_{\perp}}{\partial r} + \frac{n}{r} \frac{\sigma_{\perp} - \sigma_{\parallel}}{\sigma_{\perp}} \frac{A_n r^{2n} + B_n}{A_n r^{2n} - B_n} \quad (18)$$

depends upon n , as well as on the (unknown) ratios $\mathfrak{R}_n(r) = B_n/A_n$. These ratios, in turn, are themselves found from Eqs. (16). After further manipulation, we find

$$\frac{\partial \mathfrak{R}_n}{\partial r} = \frac{1}{2r^{2n}} \left\{ \frac{1}{\Lambda_1} [r^{4n} - \mathfrak{R}_n^2] + n \frac{1}{\Lambda_2} [r^{2n} + \mathfrak{R}_n]^2 \right\} \quad (n \neq 0). \quad (19)$$

In writing this result we have introduced the *scattering lengths* $\Lambda_{1,2}(r)$ defined by

$$\frac{1}{\Lambda_1(r)} = \frac{1}{\sigma_{\perp}} \frac{\partial \sigma_{\perp}}{\partial r}, \quad \frac{1}{\Lambda_2(r)} = \frac{1}{r} \frac{\sigma_{\perp} - \sigma_{\parallel}}{\sigma_{\perp}}. \quad (20)$$

For interface scattering $\Lambda_{1,2}(r)$ rise sharply from their minimum values at the fiber surface to become infinite in the bulk; with no interface scattering $\Lambda_{1,2}$ are everywhere infinite, and Eq. (19) prescribes \mathfrak{R}_n constant, as expected for a matrix with uniform conductivity (A_n, B_n constant).

The boundary condition on \mathfrak{R}_n follows from requiring the normal component of current density to vanish at the (nonconducting) fiber surface $r=a$. On account of Eqs. (16), the normal component of \mathbf{J} is simply proportional to $\sigma_{\perp}(r) \cdot [A_n r^{n-1} - B_n r^{-n-1}]$. At the fiber surface this will be zero only if $\mathfrak{R}_n(a) = a^{2n}$. [This result also can be recovered from Eq. (15), now taking the i th ring to lie just beneath the fiber surface.] The matrix problem then reduces to one of solving Eq. (19) for $\mathfrak{R}_n(r)$, subject to $\mathfrak{R}_n(a) = a^{2n}$. Once $\mathfrak{R}_n(r)$ is known, Eqs. (16) can be integrated immediately to get explicit results for $A_n(r)$ and $B_n(r)$ separately, in terms of their values at the fiber surface.

Before proceeding with the solution for $\mathfrak{R}_n(r)$, we should pause to establish exactly what will be needed for the calculation of the transverse composite conductivity.

Figure 3 is an exploded view of the lattice showing little more than one primitive cell. Since the scattering effect is presumed confined to the inscribed circle, the shaded regions are charge free, and the electric potential at any point such as P obeys Laplace's equation; more precisely, V_P is given by Eq. (17) with $A_n(r), B_n(r)$ evaluated at $r=b$. Along with Rayleigh, we make the following observations.

(i) V_P arises from two kinds of sources, those (at infinity) responsible for the applied field, and the distribution of charge surrounding each lattice site. The latter produces a potential at P with the periodicity of the lattice. Superimposed on this *lattice potential* is the applied field contribution, which varies linearly as P moves up and down the field direction. As a result, the potential at a point equivalent to P in the cell to the immediate left of the one shown differs from V_P only by $E \times 2b$, where E is the applied field strength.⁶ Indeed, the potential anywhere in the matrix can be referred to this second cell, and is again given by Eq. (17), with r measured from the new center. Referred to the new cell, *the coefficients A_n and B_n will be unchanged, except for A_0 , which acquires the additive constant $E \times 2B$.*

(ii) The terms in Eq. (17) which are singular at $r=0$ represent the contribution to V_P from sources within the central cell; conversely, the nonsingular terms arise from sources in the surrounding cells, together with those at infinity, as discussed above. It follows that the coefficients $A_n(b)$ in the central cell, after correcting for the potential of the applied field, can be expressed in terms of the $B_n(b)$ originating with all other cells. According to Rayleigh

$$\begin{aligned}E - A_1(b) &= B_1(b) \frac{S_2}{(2b)^2} + 3B_3(b) \frac{S_4}{(2b)^4} \\ &\quad + 5B_5(b) \frac{S_6}{(2b)^6} + \dots, \\ -A_3(b) &= B_1(b) \frac{S_4}{(2b)^4} + \left[\frac{5}{2} \right] B_3(b) \frac{S_6}{(2b)^6} + \dots, \\ -A_5(b) &= B_1(b) \frac{S_6}{(2b)^6} + \left[\frac{7}{2} \right] B_3(b) \frac{S_8}{(2b)^8} + \dots.\end{aligned}\quad (21)$$

In effect, Eqs. (21) express the boundary conditions imposed by the surrounding (square) lattice. The *lattice sums* S_n are pure numbers characterizing the lattice geometry.⁷

To obtain the transverse conductivity, we apply Green's theorem

$$\int \left[U \frac{\partial V}{\partial n} - V \frac{\partial U}{\partial n} \right] ds = 0 \quad (22)$$

to the contour bounding the shaded region in Fig. 3. Within this region V satisfies Laplace's equation, as does U if we take $U = x = r \cos \theta$. On the circular (inner) part of the contour, only the terms with $n=1$ in Eq. (17) contribute, and we find for this part of the integral $2\pi B_1(b)$. For the square (outer) part, there is no contribution from the top or bottom edges, since $\partial V / \partial n, \partial U / \partial n$ both van-

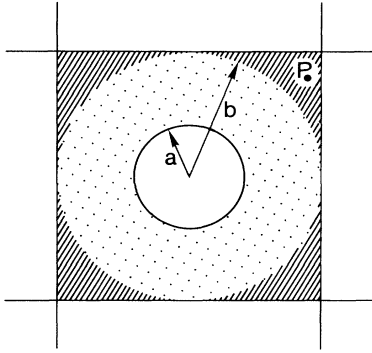


FIG. 3. Exploded view of the lattice showing a single representative cell. The scattering effect is presumed confined to the inscribed cylinder, leaving the shaded regions charge free. The potential at any point such as P obeys Laplace's equation.

ish there. For the remainder, we note that $\sigma_0 \int \partial V / \partial n ds$ is the total current I across the cell, while U and V change by $2b$ and $E \times 2b$, respectively, over the dimension of the cell. Putting it all together, we find

$$2\pi B_1(b) + 2b \frac{I}{\sigma_0} - 2b(E \times 2b) = 0. \quad (23)$$

The transverse conductivity of the specimen is $I/E \times 2b$, or

$$\frac{\sigma_t}{\sigma_0} = 1 - \frac{2\pi B_1(b)}{(2b)^2 E}. \quad (24)$$

The ratio $B_1(b)/E$ is found from Eqs. (21). In lowest approximation, S_4, S_6, \dots are neglected to get $(2b)^2 E/B_1(b) = (2b)^2/\mathfrak{R}_1(b) + S_2$. A much better result obtains if we keep S_4 ($S_6=0$ for square order); then $(2b)^2 E/B_1(b) = (2b)^2/\mathfrak{R}_1(b) + S_2 - 3(2b)^{-6}\mathfrak{R}_3(b)S_4^2$ and

$$\frac{\sigma_t}{\sigma_0} = 1 - 2\pi \frac{1}{(2b)^2 \mathfrak{R}_1^{-1}(b) + S_2 - 3(2b)^{-6} \mathfrak{R}_3(b) S_4^2}. \quad (25)$$

Equation (25) is accurate up to and including the quadrupole term, and requires \mathfrak{R}_1 —as well as \mathfrak{R}_3 —evaluated at $r=b$. Inclusion of the next (octupole) term would necessitate $\mathfrak{R}_5(b)$, etc.

For the ratios \mathfrak{R}_n we return to Eq. (19) and introduce the deviates $\delta\mathfrak{R}_n(r) = \mathfrak{R}_n(r) - a^{2n}$, subject to $\delta\mathfrak{R}_n(a) = 0$. Without interface scattering $\delta\mathfrak{R}_n(r)$ is everywhere zero; accordingly, we linearize Eq. (19) in the (small) quantities $\delta\mathfrak{R}_n$. This linearized version can be integrated in terms of the integrating factor

$$\ln I_n = a^{2n} \int_a^r \left\{ \frac{1}{\Lambda_1} - \frac{n}{\Lambda_2} \frac{r^{2n} + a^{2n}}{a^{2n}} \right\} \frac{dr}{r^{2n}} \quad (26)$$

$$\delta\mathfrak{R}_n(b) = \frac{4n}{k} a^{2n} \left\{ z - \frac{\frac{3}{8\pi} [E_5(z) - E_3(z) + \frac{1}{4}]}{1 - \frac{3}{2} E_4(z)} \right\}_{z=(b-a)/\lambda}. \quad (29)$$

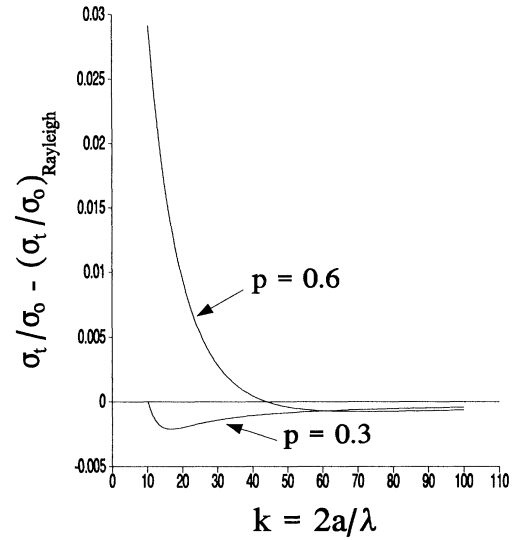


FIG. 4. Scattering correction to the transverse conductivity σ_t as a function of $k=2a/\lambda$ for composites with 30% and 60% fiber by volume. The correction is surprisingly small, and comparable to that found in the longitudinal orientation.

to get

$$\begin{aligned} \frac{\delta\mathfrak{R}_n(r)}{2na^{2n}} \approx & \int_1^{r/a} \left[1 - \frac{I_n(\rho a)}{I_n(r)} \right] \rho^{4n-1} d\rho \\ & + \frac{a}{4} \int_1^{r/a} \frac{I_n(\rho a)}{I_n(r)} \frac{(\rho^{2n} + 1)^2}{\Lambda_2(\rho a)} d\rho. \end{aligned} \quad (27)$$

To make further progress, we introduce $z=d(r)/\lambda = (r-a)/\lambda$, the natural variable for interface scattering in this cylindrical geometry, and observe that, since the main contributions to the integrals come from the lower limit, Eqs. (26) and (27) afford asymptotic developments for $\ln I_n$ and $\delta\mathfrak{R}_n$, respectively, in inverse powers of $k=2a/\lambda$:

$$\ln I_n = \ln \sigma_{\perp}(r) - \ln \sigma_{\perp}(a) + O \left[\frac{1}{k} \right], \quad (28)$$

$$\frac{\delta\mathfrak{R}_n}{2na^{2n}} = \frac{2}{k} \int_0^z \left[1 - \frac{\sigma_{\parallel}(z')}{\sigma_{\perp}(z)} \right] dz' + O \left[\frac{1}{k^2} \right].$$

The surviving integral for $\delta\mathfrak{R}_n$ has already been encountered in our study of the longitudinal conductivity. For this, the transverse case, we evaluate the result at $r=b$ to get

There is one feature of our result which deserves special mention: in some composite applications $\mathfrak{R}_n(b)$ can be negative, leading to a transverse conductivity for the composite which may become *higher* than the matrix value alone. This seemingly paradoxical result evidently stems from a complex redistribution of current flow within the sample, and is intimately related to the tensor character of the effective conductivity: indeed, for scalar functions $\sigma(r)$, $\Lambda_2 = \infty$ and Eq. (19) prescribes ratios $\mathfrak{R}_n(r)$, which increase monotonically from their values at the fiber surface.

Figure 4 shows the scattering correction to the transverse conductivity given by Eqs. (25) and (29), as a function of $k = 2a/\Lambda$ for samples containing 30% and 60%

fiber by volume. (Recall that for typical B-Al composites, $k \sim 100$ at room temperature and decreases with decreasing temperature.) At 60% fiber concentration, interface scattering has the expected effect for k in excess of about 50; below this value anomalous behavior sets in, with the sample conductivity exceeding the matrix value when $k \leq 44$. At the 30% fiber level, the onset of anomalous behavior does not occur until $k \sim 16$, a value not likely to be reached experimentally—at least for the B-Al composites, where grain sizes are thought to limit the mean free path to less than about $10 \mu\text{m}$.

Again, the only simple result for the transverse conductivity is that which obtains in the case $\lambda \ll b - a$:

$$\frac{\sigma_t}{\sigma_0} = 1 - \frac{2p}{\left[1 + \frac{3}{8\pi k}\right]^{-1} + p - 3p^4 \pi^4 (0.03235020)^2 \left[1 + \frac{9}{8\pi k}\right]}, \quad (30)$$

Significantly, Eq. (30) does not predict the anomaly discussed in the preceding paragraph, indicating that the strange effect is not only tensor related, but also manifest only when $\lambda \sim b - a$, i.e., at very low temperatures and/or high fiber content. (For both curves shown in Fig. 4, the scattering correction drops to zero at $b - a \approx 3\lambda$.)

Finally, over the entire “normal” range, we see that the scattering correction to the transverse conductivity is quite small, and does not differ appreciably from the values found in the longitudinal orientation. In this respect the treatment has failed to provide a quantitative explanation for the abnormally small transverse conductivity (high resistivity) observed in the B-Al composites containing 60% boron fiber.

IV. SUMMARY AND CONCLUSIONS

The methods exhibited here represent sophisticated analytical efforts to assess the effect of interface scattering on the conductivity of metal-matrix composites. Our work is subject to two important limitations: (1) The effective conductivity for scattering, Eq. (1), used in our computations is valid only for fiber diameters large compared to the bulk mean free path. This sets a lower limit on k (~ 1), below which the predictions of our model are unreliable. (2) Every fiber is assumed to scatter independently of its neighbors, implying that the scattering effect of each fiber is confined to its representative cell and does not “spill over” into adjacent cells. This sets a lower limit on $(b - a)/\lambda$ in our model (again, ~ 1), and tends to be the more restrictive of the two conditions. We note,

however, that this limitation is shared by *all* existing theories.

In the longitudinal orientation, Eq. (10) would appear to cover most cases of practical interest; the more complicated Eq. (11) is essential only in applications involving low temperatures and/or high fiber volume fractions. The scattering correction to the longitudinal conductivity tends to be small ($\leq 1\%$); in no instance do we find the abnormally large values predicted by previous theory (though not observed).

Results for the transverse orientation are understandably more difficult to obtain, and more complex. The simpler Eq. (30) should be applicable in many situations, but does not incorporate the predicted anomaly associated with the tensor aspects of conduction in metal-matrix composites. The scattering correction to the transverse conductivity is surprisingly small, and comparable to that found in the longitudinal orientation. As such, the model fails quantitatively to explain the unusually low transverse conductivity (high resistivity) reported for B-Al composite with 60% boron fiber. This failure may be rooted in the Rayleigh approach, which represents the composite electric field as a multipole series (truncated at the quadrupole term). For high fiber content the series converges very slowly, and no finite number of terms can account for the singularity at $\approx 78\%$ fiber content (where adjacent fibers touch, blocking all conducting paths). Keller⁸ has shown how to describe this singularity analytically, and a logical extension of the present work would attempt to include the scattering effect in Keller’s treatment.

¹D. Abukay, K. V. Rao, S. Araj, and Y. D. Yao, *Fiber Sci. Tech.* **10**, 313 (1977). Data and analysis for other composites in the same series may be found in the doctoral thesis of K. W. Tse, *Electrical Conductivities of Fiber Reinforced Composites* (University Microfilms International, Ann Arbor, MI, 1984), Chap. 4.

²F. S. Roig and J. E. Schoutens, *J. Mater. Sci.* **21** 2409 (1986). Subsequently, a correction appeared by the same authors in *J. Mater. Sci.* **22**, 4002 (1987).

³C. A. Moyer, S. Araj, Y. D. Yao, and Y. Y. Chen, *Phys. Status Solidi A* **120**, K71 (1990).

⁴C. A. Moyer, preceding paper, *Phys. Rev. B* **47**, 10 079 (1993).

⁵J. W. Rayleigh, *Philos. Mag.* **34** (5), 481 (1892).

⁶This identification of the local field E with the applied field assumes the sample is infinitely elongated in the field direction.

⁷For square order, Rayleigh has given the results $S_2 = \pi$, $S_4 = \pi^4 \times 0.032\,350\,20$, and $S_{2n} = 0$ whenever n is otherwise

odd (S_6, S_{10} , etc.). S_2 is actually shape dependent; the given value is for a sample infinitely elongated in the field direction (cf. Ref. 6 above).

⁸J. B. Keller, *J. Appl. Phys.* **34** (4), 991 (1963).